



Magmatic evolution of the differentiated ultramafic, alkaline and carbonatite intrusion of Vuoriyarvi (Kola Peninsula, Russia). A LA-ICP-MS study of apatite

S. Brassinnes^{a,*},¹, E. Balaganskaya^b, D. Demaiffe^a

^aUniversité Libre de Bruxelles, Géochimie isotopique (CP160/02), 50 Av. Roosevelt, 1050 Bruxelles, Belgium

^bGeological Institute, Kola Science Centre RAS, Fersman Street 14, Apatity 184209, Russia

Received 12 January 2004; accepted 11 March 2005

Available online 20 June 2005

Abstract

The nature of the petrogenetic links between carbonatites and associated silicate rocks is still under discussion (i.e., [Gittins J., Harmer R.E., 2003. Myth and reality of the carbonatite–silicate rock “association”. *Period di Mineral.* 72, 19–26.]). In the Paleozoic Kola alkaline province (NW Russia), the carbonatites are spatially and temporally associated to ultramafic cumulates (clinopyroxenite, wehrlite and dunite) and alkaline silicate rocks of the ijolite–melteigite series [Kogarko, L.N., 1987. Alkaline rocks of the eastern part of the Baltic Shield (Kola Peninsula). In: Fitton, J.G., and Upton, B.G.J. (eds). *Alkaline igneous rocks*. Geol. Soc. Special Publication 30, 531–544; Kogarko, L.N., Kononova, V.A., Orlova, M.P., Woolley, A.R., 1995. *Alkaline rocks and carbonatites of the world. Part 2. Former USSR*. Chapman and Hall, London, 225 pp; Verhulst, A., Balaganskaya, E., Kirmarsky, Y., Demaiffe, D., 2000. Petrological and geochemical (trace elements and Sr–Nd isotopes) characteristics of the Paleozoic Kovdor ultramafic, alkaline and carbonatite intrusion (Kola Peninsula, NW Russia). *Lithos* 51, 1–25; Dunworth, E.A., Bell, K., 2001. The Turiy Massif, Kola Peninsula, Russia; isotopic and geochemical evidence for a multi-source evolution. *J. Petrol.* 42, 377–405; Woolley, A.R., 2003. Igneous silicate rocks associated with carbonatites: their diversity, relative abundances and implications for carbonatite genesis. *Period. di Mineral.* 72, 9–17]. In the small ($\approx 20 \text{ km}^2$) Vuoriyarvi massif, apatite is typically a liquidus phase during the magmatic evolution and so it can be used to test genetic relationships. Trace elements contents have been obtained for both whole rocks and apatite (by LA-ICP-MS). The apatites define a single continuous chemical evolution marked by an increase in REE and Na (belovite-type of substitution, i.e., $2\text{Ca}^{2+} = \text{Na}^+ + \text{REE}^{3+}$). This evolution possibly reflects a fractional crystallisation process of a single batch of isotopically homogeneous, mantle-derived magma.

The distribution of REE between apatite and their host carbonatite have been estimated from the apatite composition of a carbonatite vein, belonging to the Neskevara conical-ring-like vein system. This carbonatite vein is tentatively interpreted as a melt. So, the calculated distribution coefficients are close to partition coefficients. Rare earth elements are compatible in

* Corresponding author. Tel.: +32 2 6502246; fax: +32 2 6502226.

E-mail address: stephane.brassinnes@ulb.ac.be (S. Brassinnes).

¹ FRIA Grant.

apatite ($D > 1$) with a higher compatibility for the middle REE ($D_{Sm}: 6.1$) than for the light ($D_{La}: 4.1$) and the heavy ($D_{Yb}: 1$) REE.

© 2005 Elsevier B.V. All rights reserved.

Keywords: Carbonatite; Kola; Apatite; LA-ICP-MS; Fractional crystallisation

1. Introduction

In some alkaline intrusions, carbonatites are associated in space and time with a diversity of igneous alkalic silicate rocks (i.e., Woolley, 2003; Gittins and Harmer, 2003 for recent reviews). The genetic relationships between these silicate rocks and the carbonatites remain unclear (see discussion in Gittins and Harmer, 2003). Does this association reflect a petrogenetic link (differentiation of a single batch of melt) or only the spatial juxtaposition of two independent magma batches? In the Paleozoic ultramafic, alkaline and carbonatite province of the Kola Peninsula (Russia), carbonatites occur as dykes or magmatic bodies crosscutting the ultramafic cumulates and the alkaline silicate rocks of the ijolite–melteigite series.

Immiscibility between a carbonate-rich liquid and an alkaline silicate liquid has often been invoked to explain the close spatial association between carbonatite and syenite (or phonolite) (i.e., Lee and Wyllie, 1996). Experimental work (Lee and Wyllie, 1998) on the complex $\text{CaO-Na}_2\text{O-(MgO+FeO)-(SiO}_2+\text{Al}_2\text{O}_3\text{)-CO}_2$ system shows that a miscibility gap can be reached during crystallisation of a parental carbonated-silicate melt, depending on the system parameters (P, T, x).

This paper is focused on the small differentiated Vuoriyarvi (=Vuorijarvi) massif. Whole rock geochemical data (trace elements) on the silicate rocks and on the carbonatites as well as trace element compositions obtained on apatites by laser ablation coupled to an ICP-MS are presented and discussed to better constrain the possible petrogenetic relations between the silicate rocks and the carbonatites. We also attempt to estimate the REE partition coefficients between apatite and carbonatite melt. Two recent papers on the REE partition coefficients between apatite and carbonatite melt (the model calculation of Bühn et al., 2001, from magmatic fluorapatite of African carbonatites on one hand and the experimen-

tal work of Klemme and Dalpé, 2003, on the other hand) give contrasting results.

2. Geological setting

The Kola Peninsula (north-western Russia) consists of three Archean terranes (or blocks) reworked to different extent during the Palaeoproterozoic: the Murmansk terrane, the Central Kola Composite terrane and the Belomorian terrane (Kratz et al., 1978; Mitrofanov, 1995). These terranes form the north-eastern part of the Baltic Cratonic Shield and are separated by granulite belts and listric first-order faults. The Kola Alkaline and Carbonatite Province (i.e., Kogarko, 1987; Kogarko et al., 1995) of Late Devonian (380–360 Ma) age (Kramm et al., 1993) comprises numerous ultramafic, alkaline and carbonatite intrusions and the two giant agpaitic nepheline syenite massifs of Khibiny (=Khibina) and Lovozero. The massifs were emplaced along reactivated NW–SE Proterozoic lineaments (i.e., the Kandalaksha Deep Fracture Zone, the Kontozero Graben) and the associated Riedel fractures (Balagansky et al., 1996).

The Vuoriyarvi intrusion (Fig. 1) is a small (3.5×5.5 km, about 20 km²) elliptical massif cross-cutting the Archean (2.9 Ga) Belomorian gneisses (i.e., Timmerman and Daly, 1995 and references therein). An isotopic study on the Vuoriyarvi massif has given a range of intrusion age (Rb–Sr mineral isochrons) between 375 ± 7 and 383 ± 7 Ma (Gogol and Delinitzin, 1999). The massif has a concentrically zoned structure classically interpreted as resulting from several magma pulses. The core zone (≈ 12 km²) is made of ultramafic cumulates, mainly clinopyroxenites (grading to nepheline-bearing clinopyroxenites towards the rims) with rare lenses of wehrlites and dunites (=olivinite of the Russian authors; i.e., Kukhareenko et al., 1965). The outer rim of the massif is represented by alkaline

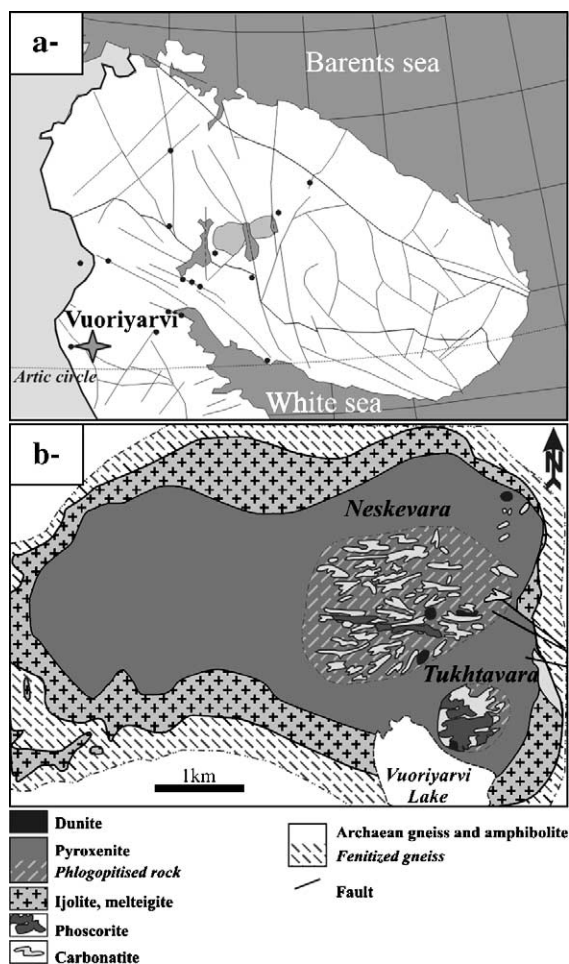


Fig. 1. a) Localisation of the Vuoriyarvi massif in the Kola Peninsula. b) Schematic map of the Vuoriyarvi massif (after Kukharensko et al., 1965), lithologies in italic letters are transformed rocks.

rocks of the ijolite–melteigite series, some ijolites being partly recrystallised (autometamorphism). Carbonatites occur as sheets and dykes and as two stockworks in the eastern part of the massif: the “Neskevara” and the “Tukhtavara” stockworks. Forsterite-, magnetite-, apatite-rich rocks (i.e., phoscorites sensu Russel et al., 1954) are intimately associated with carbonatites. These phoscorites usually appear as coarse-grained, very heterogeneous rocks in hand specimens. It is not possible to collect representative samples for geochemical purposes. The phoscorites were thus not studied in this paper. The country rocks have been intensively fenitized over several hundreds of meters.

3. Petrographic description

Only a short description is given below (for more details, see Brassinnes et al., 2003).

3.1. Ultramafic rocks

The ultramafic rocks which constitute the core of the Vuoriyarvi massif are mainly clinopyroxenites; more rarely wehrlite and dunite. The clinopyroxenites display typical cumulate texture, varying from orthocumulate to mesocumulate. The essential cumulus mineral is diopside with subsidiary olivine (Fo87), perovskite and apatite. The interstitial (=intercumulus) space is filled with anhedral, locally poikilitic, phlogopite, magnetite, nepheline/cancrinite and calcite. Apatite is locally in equilibrium within anhedral nepheline (Fig. 2a); elsewhere it occurs as polygonal grains concentrated in segregation pockets filling fractures. At the periphery of the ultramafic central zone, the clinopyroxenites are enriched in interstitial liquid that has crystallised as anhedral nepheline grains.

3.2. Alkaline silicate rocks of the ijolite–melteigite series

Most of the samples studied are ijolites; melteigites are much less common. Two families of ijolite have been distinguished: 1) cumulates with large (few mm) euhedral, slightly zoned, aegirine–augite crystals surrounded by subhedral nepheline associated with magnetite (and schorlomite); 2) ijolites with euhedral, complexly zoned aegirine–augite and large euhedral titanite included in a fine-grained matrix (some tens of μm) made of nepheline and cancrinite. Locally, large subhedral nepheline grains are granulated to small subgrains that grade into the fine-grained matrix. Apatite (up to >1 mm) is present in both types of ijolite as subhedral grains located either in the interstitial space between the aegirine–augite grains (Fig. 2b) or in the fine-grained matrix.

3.3. Carbonatite

Several generations of carbonatite (named CI to CIV) have been described by Kapustin (1980). Only the apatite-bearing carbonatites of the early stages CI and CII are briefly described in this paper. They are

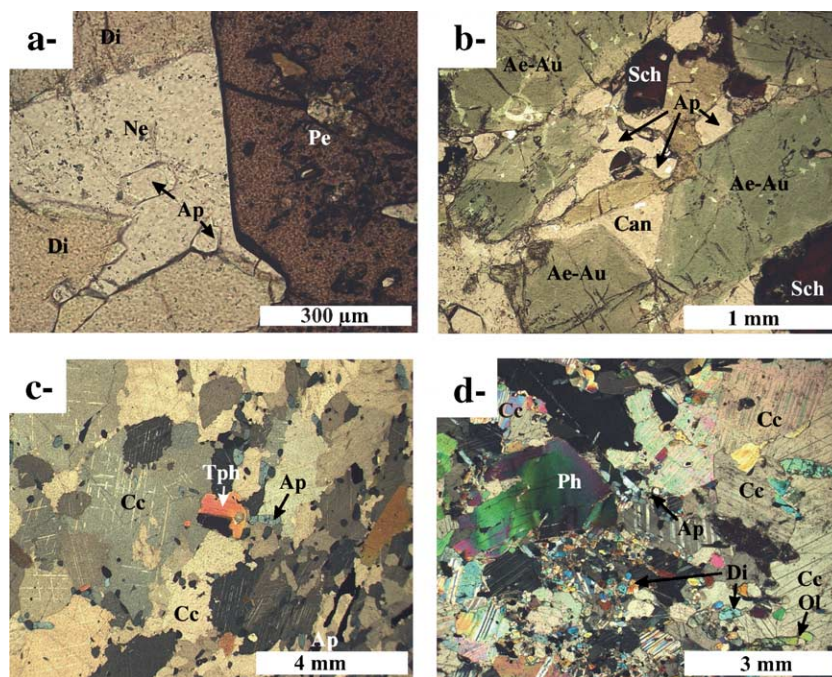


Fig. 2. Microphotographs of the main lithologies of the Vuoriyarvi massif. a) Clinopyroxenite (VJA74) with cumulus diopside and perovskite; the interstitial space is filled with euhedral apatite and anhedral nepheline—natural light; b) General view of ijolite (VJA71) with subhedral apatite grains between large aegirine–augite crystals, schorlomite and cancrinite—natural light; c) Apatite- and tetraferriphlogopite-bearing carbonatite (BR64)—crossed nicols; d) Silicate-rich (forsterite, diopside, phlogopite) and apatite-bearing carbonatite (BR18)—crossed nicols. (Di: diopside, Ap: apatite, Pe: perovskite, Ne: nepheline, Ae–Au: aegirine–augite, Can: cancrinite, Sch: schorlomite, Ph: phlogopite, Ol: olivine, Cc: calcite and Tph: tetraferriphlogopite).

generally calciocarbonatite and occur in the field as stocks and/or in a conical-ring-like vein system. They can be rich in accessory silicates (forsterite, diopside, phlogopite/tetraferriphlogopite), in euhedral apatite (generally of mm size but occasionally up to 1 cm), and in oxides (magnetite, pyrochlore, . . .).

Sample BR64, which belongs to the Neskevara conical-ring-like vein system, only contains tetraferriphlogopite, apatite, magnetite and calcite (Fig. 2c). The calcite grains are generally anhedral, but slightly elongated and display consertal textures. Euhedral apatite displays strong preferred orientation (magmatic flow texture?). This sample is tentatively interpreted as a rapidly crystallised melt. It is indeed petrographically very similar to thin (≈ 1 cm) carbonatite veinlets that are obviously much closer to a quenched melt than to a magmatic body.

Sample BR18, from the Tukhtavara stock, contains olivine, magnetite, phlogopite, diopside (Fig. 2d). Subhedral apatite, olivine and diopside are not orien-

tated and are engulfing anhedral calcite (interstitial material?). Petrographic status of this carbonatite (melt or cumulate) is difficult to assess.

Locally, large (≈ 1 mm) fragmented dark-brownish pyrochlore crystals containing numerous calcite inclusions have been observed (i.e., sample BR30).

4. Analytical techniques

Major and trace (Y, Nb, Ta and the REEs) elements were determined for whole rock samples (Table 1) by inductively coupled plasma emission mass spectrometry (ICP-MS) at the “Musée Royal de l’Afrique Centrale, Département de Géologie”, Tervuren, Belgium using a VG Elemental Plasma Quad instrument. Details of the analytical procedure have been given by André and Aschepkov (1996). The precision of the measurements is generally better than $\pm 5\%$ for concentrations ≥ 1 ppm.

Table 1

a) Whole rock analyses (major and trace elements) of representative clinopyroxenites (P), ijolites (A) and carbonatites (C) of the Vuoriyarvi massif; b) Average major element compositions (wt.%) of the apatites (bdl=below detection limits)

(a)										
Sample	VJA 45	VJA 60	VJA 73	VJA 74	VJA 71	VJA 72	BR 18	BR 30	BR 35	BR 64
Rock type	P	P	P	P	A	A	C	C	C	C
<i>Major elements (wt.%)</i>										
SiO ₂	41.07	36.99	36.03	39.11	34.70	35.48	7.01	2.23	2.49	1.25
TiO ₂	2.94	4.51	5.26	2.33	1.88	3.24	0.29	0.08	0.12	0.08
Al ₂ O ₃	5.33	3.31	4.24	2.84	13.42	16.04	0.81	0.03	0.40	0.31
Fe ₂ O ₃	8.17	14.10	8.34	7.25	6.75	6.80	2.35	0.54	1.01	2.57
FeO	4.97	7.64	5.99	4.36	4.08	4.38	1.62	1.37	0.86	2.05
MnO	0.17	0.20	0.22	0.17	0.25	0.23	0.17	0.25	0.10	0.12
MgO	12.41	12.70	10.41	11.16	3.96	3.51	4.17	2.43	2.57	1.84
CaO	21.24	17.95	22.32	26.05	15.70	11.10	45.38	49.39	52.09	52.19
Na ₂ O	0.97	0.61	1.19	0.67	9.56	11.22	0.30	0.32	0.09	0.11
K ₂ O	0.86	0.62	1.05	0.21	0.56	0.72	0.57	0.25	0.23	0.26
P ₂ O ₅	0.31	0.03	3.39	4.74	2.37	0.52	4.36	5.79	1.74	3.41
PF	1.39	0.90	1.31	0.57	5.44	5.51	33.34	37.03	38.71	36.65
Total	99.83	99.57	99.76	99.46	98.66	98.76	100.37	99.73	100.40	100.84
<i>Trace elements (ppm)</i>										
Nb	97.0	47.0	388.0	48.0	221.0	437.0	53.0	1300.0	47.0	10.0
Ta	11.1	4.2	25.0	4.2	47.0	103.0	6.7	1.3	6.7	0.6
Y	22.0	20.0	49.0	34.0	88.0	35.0	121.0	79.0	67.0	41.0
La	97.0	55.0	392.0	113.0	162.0	113.0	368.0	482.0	300.0	147.0
Ce	235.0	118.0	729.0	208.0	406.0	314.0	793.0	996.0	609.0	306.0
Pr	30.0	15.1	82.0	25.0	56.0	47.0	103.0	125.0	73.0	39.0
Nd	111.0	58.0	286.0	96.0	234.0	187.0	391.0	449.0	269.0	146.0
Sm	15.9	9.5	42.0	16.1	43.0	30.0	63.0	60.0	39.0	23.0
Eu	4.3	2.8	12.7	5.0	13.3	8.7	19.4	17.3	11.8	6.6
Gd	10.7	7.6	31.0	13.5	35.0	19.9	51.0	42.0	30.0	17.3
Dy	5.0	4.0	15.3	7.3	22.0	9.6	30.0	19.8	16.0	9.1
Ho	0.7	0.6	2.2	1.1	3.8	1.3	4.9	3.1	2.5	1.4
Er	1.4	1.1	3.9	2.2	8.2	2.6	10.4	6.1	5.1	3.1
Yb	0.9	0.6	1.7	1.2	5.4	1.4	6.2	3.7	3.0	1.9
Lu	0.1	0.1	0.2	0.1	0.7	0.2	0.8	0.5	0.3	0.2
∑REE	1547.8	510.5	2392.7	721.5	1730.2	1743.7	2163.4	3617.2	1671.9	870.0
(La/Yb) _N	70.9	59.3	161.4	64.0	20.4	53.3	40.3	88.5	67.9	53.4
(b)										
Sample	VJA74		VJA71		BR 18		BR 35		BR 64	
Rock type	P		A		C		C		C	
	(n=13)	2*S.D.	(n=8)	2*S.D.	(n=10)	2*S.D.	(n=14)	2*S.D.	(n=15)	2*S.D.
SiO ₂	0.69	0.25	0.76	0.39	1.16	0.06	1.22	1.16	0.13	0.11
FeO	0.06	0.11	0.09	0.14	0.04	0.06	0.01	0.05	bdl	0.07
MnO	0.04	0.10	0.02	0.05	0.01	0.05	bdl	–	bdl	–
CaO	56.03	1.10	55.85	1.33	55.31	0.31	55.11	0.83	56.22	0.61
Na ₂ O	0.07	0.08	0.12	0.04	0.06	0.02	0.14	0.15	0.17	0.11
P ₂ O ₅	39.27	0.77	40.19	0.67	39.21	0.63	39.10	2.25	42.35	0.84
La ₂ O ₃	0.02	0.04	0.21	0.06	0.25	0.07	0.31	0.18	0.05	0.02
Ce ₂ O ₃	0.08	0.16	0.57	0.24	0.56	0.08	0.80	0.36	0.11	0.04
F	1.26	0.11	1.68	0.16	2.86	0.60	2.87	1.07	2.55	0.73

Table 1 (continued)

(b)										
Sample	VJA74		VJA71		BR 18		BR 35		BR 64	
Rock type	P		A		C		C		C	
	(n=13)	2*S.D.	(n=8)	2*S.D.	(n=10)	2*S.D.	(n=14)	2*S.D.	(n=15)	2*S.D.
Cl	bdl	–	bdl	–	bdl	–	bdl	–	bdl	–
O=F	–0.53		–0.71		–1.20		–1.21		–1.07	
O=Cl	–		–		–		–		–	
Total	96.98		98.77		98.25		98.36		100.50	

Mineral compositions have been obtained by electron microprobe (Camebax Microbeam instrument at the University of Nancy I, France) operating at an accelerating voltage of 15 kV, a beam current of 10 nA and a counting time per element of 10 s for major elements and 20 s for trace elements. For accessory minerals, a bivoltage program was used, giving 15 kV for major elements and 20 kV for trace elements. Standards used were a combination of natural and synthetic minerals and data correction was by a ZAF method (Henoc and Tong, 1978). Apatite average compositions are given in Table 1.

Trace elements (and more specifically the rare earth elements and Y) were analysed in apatite from ultramafic rocks, alkaline silicate rocks and carbonatites using in situ LA-ICP-MS. The data were collected with a UV Fisons laser ablation microprobe coupled to a VG Elemental Plasma Quad (PQ2 Turbo Plus) ICP-MS (Musée Royal de l'Afrique Centrale, Tervuren). Representative data and ranges of variations are given in Table 2. The laser microprobe used in this study is based on a continuum Minilite Q-switched Nd:YAG laser operating in the far-UV (266 nm) wavelength. The power of the output beam is maximum (2 mJ/pulse) for a 10 Hz repetition rate of pulse, that is attenuated in agreement with the appropriate energy to the crater size requirement. The craters are in the range 40–60 μm . The focusing on the sample is done manually through a high magnification lens (1500 \times). Each sample and standard was ablated for 27 s corresponding to 12 s of pre-ablation, followed by 15 s of data acquisition. The raw data on each isotope peak were subtracted from the gas blanks and normalised to the ^{43}Ca signal and then compared to calibration lines. The calibration lines are based on the NIST 612 and NIST 610

glasses and on a laboratory apatite standard (an unzoned apatite from Madagascar) to constrain the matrix effects. Typical theoretical detection limits for semi-quantitative analyses ($>$ background+3 σ) are in the range 30–300 ppb for Y, La, Ce, Pr, Eu, Sm, Gd, Ho, Lu, 500 ppb–1.25 ppm for Nd, Dy, Er and Yb. The limits for quantitative analyses are greater, 300 ppb–2.40 ppm for Y, La, Ce, Pr, Eu, Sm, Gd, Ho, Er, Lu, 3.50–4.50 ppm for Nd, Dy and Yb. The typical precision and accuracy for a laser microprobe analysis (calculated on 10 analyses on NIST612 and NIST610 glasses and on 17 analyses on laboratory apatite standard) range from 3–11% for NIST612, from 5–12% for NIST610 and from 7–15% for the laboratory apatite standard.

5. Results

Before the discussion of the trace elements contents in apatite, it seems useful to summarize the whole rock geochemical data (spidergrams, REE plots) that have been briefly presented by Brassinnes et al. (2003).

5.1. Trace elements geochemical data of whole rocks

Only samples that have homogeneous grain size and that do not present any evidence of brecciated texture and/or mixed material were selected for whole rock analyses. Ten c.a. 500 g fresh samples (4 clinopyroxenites, 2 ijolites and 4 carbonatites) have been analysed.

The four clinopyroxenites display large ranges of trace elements content: i.e., ΣREE varies from 510 to 2392 ppm with $(\text{La}/\text{Yb})_{\text{N}}$ in the range 60–160; Nb in the range 47–98 ppm with one perovskite-

Table 2

Trace element compositions and average composition of the apatites from the Vuoriyarvi massif (bdl=below detection limits)

Sample	Clinopyroxenite VJA74																Avge	2 S.D.
Petrography	Disseminated										Segregation pocket						<i>n</i> =49	
Grain <i>n</i> ^o	1	1	2	2	3	4	4	4	5	6	7	7	8	9	10	11		
Position	Core	Rim	Core	Rim	Core	Core	Rim 1	Rim 2	Core	Core	Core	Rim	Core	Core	Core	Core		
La	435.5	356.3	724.0	335.0	369.8	383.9	339.7	335.0	371.7	398.7	933.3	852.3	559.9	799.7	652.0	772.2	578.0	376.8
Ce	659.1	458.9	996.8	448.7	526.9	548.0	446.7	448.7	563.9	530.2	1650.3	1360.9	917.6	1319.3	974.8	1191.6	905.0	689.8
Pr	73.6	52.0	112.0	52.7	61.3	63.6	55.6	52.7	61.2	64.9	206.9	172.1	106.9	157.2	129.6	152.7	109.0	87.1
Nd	280.9	194.5	401.3	212.2	247.3	230.9	212.8	212.2	243.1	249.8	729.8	660.2	404.0	593.9	461.3	558.2	408.0	319.9
Sm	60.0	38.7	69.5	45.8	47.7	46.9	44.2	45.8	51.3	52.4	101.3	92.5	61.7	90.0	73.6	85.4	67.0	36.7
Eu	17.5	12.8	18.5	15.8	16.0	15.7	14.6	15.8	14.6	18.0	27.7	23.9	18.6	23.7	21.8	22.9	19.0	8.3
Gd	56.7	35.9	49.4	45.5	46.3	42.9	47.5	45.5	48.2	53.9	65.5	63.3	53.8	67.2	60.8	68.3	53.0	20.5
Dy	28.8	21.2	29.8	25.7	29.7	28.8	28.4	25.7	26.5	30.4	26.0	30.9	28.3	31.4	29.4	37.2	28.0	8.6
Ho	5.3	4.0	5.2	5.0	5.5	5.5	4.8	5.0	5.2	5.6	4.8	4.9	5.1	5.9	4.9	5.7	5.0	1.3
Er	8.0	6.1	8.5	8.7	8.1	8.8	7.1	8.7	6.8	9.5	6.3	7.7	7.6	8.6	7.2	9.3	8.0	2.8
Yb	4.1	2.6	5.1	3.8	3.7	4.4	2.7	3.8	3.0	4.6	bdl	2.4	2.3	4.3	3.8	3.3	3.0	2.2
Lu	0.6	0.3	0.5	0.8	0.8	0.5	bdl	0.8	bdl	0.4	bdl	0.4	0.6	0.6	bdl	0.4	bdl	–
Sr	3270.2	4112.5	4224.5	3685.4	3599.8	3638.3	3369.0	3685.4	2935.4	3818.6	3619.2	3616.9	3762.6	3677.4	3634.3	3727.1	3716.0	465.6
Y	140.1	113.4	137.7	134.6	142.9	137.8	127.6	134.6	126.7	155.2	116.6	142.6	131.2	139.7	125.7	150.0	139.0	33.5
∑REE	1630.1	1183.3	2420.5	1199.8	1363.3	1380.0	1203.9	1199.8	1395.5	1418.4	3753.0	3271.5	2166.4	3101.8	2419.2	2907.2	2183.0	1545.0

Sample	Ijolite VJA71																Avge	2 S.D.
Grain <i>n</i> ^o	1	1	2	2	3	3	4	4	5	5	6	6	7	7	8	8	<i>n</i> =27	
Position	Core	Rim	Core	Rim	Core	Rim	Core	Rim	Core	Rim	Core	Rim	Core	Rim	Core	Rim		
La	1885.6	1812.3	2305.2	2305.0	1828.7	1952.6	1980.8	2057.7	2143.4	2105.1	2105.3	2089.6	2234.4	2169.1	2017.6	1938.0	1997.0	364.2
Ce	4044.7	3941.8	5007.0	4882.9	3887.6	4019.4	4100.8	4171.2	4677.4	4370.1	4396.8	4394.3	4740.2	4772.0	4132.3	4194.1	4260.0	796.2
Pr	550.6	530.2	695.1	683.2	547.0	537.2	557.1	577.4	621.4	608.1	617.8	617.6	704.3	689.8	547.8	583.1	593.0	122.5
Nd	2185.8	2151.1	2589.2	2576.3	2154.4	2181.2	2384.9	2306.1	2437.3	2301.6	2437.7	2304.8	2590.2	2503.1	2084.5	2207.0	2307.0	358.2
Sm	327.7	394.1	382.6	394.8	327.2	332.1	396.0	359.8	388.2	341.3	349.4	351.6	389.0	368.2	313.9	330.8	358.0	52.5
Eu	83.1	106.1	103.1	103.8	85.7	89.3	107.8	91.2	99.6	89.9	98.4	93.2	103.8	92.0	84.5	88.8	94.0	16.7
Gd	206.9	264.4	242.7	232.2	204.3	213.9	268.4	214.7	241.3	215.9	217.6	200.4	245.2	225.8	191.1	208.0	220.0	42.1
Dy	93.8	141.5	101.5	94.8	92.2	99.0	145.1	97.9	101.8	102.5	91.4	87.3	97.9	96.4	78.8	90.0	101.0	32.5
Ho	16.5	22.6	16.1	14.0	14.8	16.5	24.9	16.2	14.9	14.4	15.5	14.2	15.8	14.5	13.0	14.3	16.0	5.7
Er	24.2	39.3	23.4	23.1	19.9	27.5	39.7	22.0	23.6	24.0	20.9	21.1	23.5	20.9	19.8	19.9	25.0	11.9
Yb	12.9	20.1	8.9	11.1	13.0	10.0	23.4	11.9	12.4	11.2	12.7	9.9	12.1	10.3	6.8	9.6	13.0	7.5
Lu	1.4	2.7	1.5	1.2	1.3	1.3	2.4	1.5	1.3	1.2	1.2	1.0	1.2	1.5	0.8	1.3	1.0	1.1
Sr	4398.9	4483.7	4732.2	4582.9	4370.8	5600.3	4964.2	5143.1	5185.5	4921.8	5614.2	5126.6	5135.0	4966.3	4820.5	5044.9	4778.0	907.0
Y	334.6	572.4	353.3	336.2	342.6	371.1	566.7	331.9	321.6	318.6	325.3	309.3	342.3	327.7	328.5	332.7	356.0	158.0
∑REE	9433.1	9426.2	11,476.5	11,322.4	9176.2	9480.0	10,031.3	9927.8	10,762.6	10185.2	10,364.8	10,185.0	11,157.9	10,963.7	9490.9	9684.8	9985.0	1603.0

Sample	Carbonatite BR 18											Avge <i>n</i> =13	2 S.D.	Carbonatite BR 64				
	1	1	2	3	4	5	5	6	7	8	9			1	1	2	3	3
Grain <i>n</i> °	1	1	2	3	4	5	5	6	7	8	9	1	1	2	3	3		
Position	Core	Rim	Core	Core	Core	Core	Rim	Core	Core	Core	Core	Core	Rim	Core	Core	Rim		
La	2263.8	2341.7	2615.5	2046.6	2277.9	2369.4	2343.2	2361.0	2348.1	2249.5	2381.6	2296.0	319.1	347.4	412.0	317.6	382.3	652.9
Ce	4647.2	4793.7	5436.6	4472.8	4744.3	4890.8	4892.2	4778.5	4932.4	4323.8	4871.9	4755.0	788.7	800.8	888.1	734.8	965.4	1419.9
Pr	697.4	690.3	764.4	601.9	704.2	664.6	682.0	683.5	644.4	614.4	691.4	667.0	118.5	113.6	128.6	108.8	128.7	210.7
Nd	2802.3	2643.7	2919.0	2311.5	2662.2	2751.9	2728.1	2761.4	2698.4	2454.5	2671.7	2643.0	430.0	437.4	529.9	446.0	536.0	834.0
Sm	471.5	449.7	534.6	413.8	460.6	491.0	476.2	476.0	474.5	421.4	463.4	460.0	72.6	70.2	83.5	76.5	90.9	129.1
Eu	130.5	138.9	144.8	125.5	127.8	136.0	137.0	138.8	133.7	120.9	135.3	131.0	15.7	21.9	24.8	23.1	24.4	38.9
Gd	319.4	314.3	353.3	300.6	334.2	339.1	310.0	360.7	337.0	290.7	315.2	322.0	48.2	55.2	57.8	50.1	59.8	90.0
Dy	177.6	189.0	200.2	179.7	177.8	186.4	194.4	189.5	175.3	169.3	184.4	182.0	27.0	29.0	27.5	28.7	26.8	40.6
Ho	29.7	29.8	32.3	28.1	28.7	30.4	32.3	33.6	28.8	28.9	30.4	30.0	3.5	3.5	4.2	4.2	3.9	5.7
Er	46.7	47.5	48.6	47.9	47.5	49.7	47.9	52.8	49.0	47.8	49.0	48.0	4.1	5.2	5.3	5.1	5.8	6.3
Yb	27.6	25.3	30.3	29.4	28.5	29.5	26.1	29.0	29.9	23.2	29.6	28.0	5.4	2.7	2.1	2.3	4.1	1.8
Lu	3.2	3.4	3.2	3.9	3.3	3.4	3.7	3.5	3.6	2.9	4.2	3.0	0.7	bdl	bdl	0.3	bdl	bdl
Sr	3199.6	3261.7	3240.2	3152.8	3126.9	3243.8	3115.6	3140.1	3041.3	4080.7	3316.6	3295.0	548.4	2222.5	2406.4	2109.0	2367.4	3083.4
Y	634.3	660.3	737.1	667.2	683.9	711.8	709.8	686.6	685.5	639.1	727.1	679.0	82.6	72.7	78.7	78.8	82.3	111.1
∑REE	11,616.9	11,667.4	13,082.7	10,561.8	11,596.9	11,942.1	11,873.2	11,868.3	11,855.2	10,747.1	11,828.0	11,567.0	1757.2	1887.0	2163.8	1797.5	2228.2	3430.1

Sample																	Avge <i>n</i> =40	2 S.D.
	4	5	6	6	7	8	9	10	11	12	13	13	14	15	16	16		
Grain <i>n</i> °	4	5	6	6	7	8	9	10	11	12	13	13	14	15	16	16		
Position	Core	Core	Core	Rim	Core	Core	Core	Core	Core	Core	Core	Rim	Core	Core	Core	Rim		
La	454.0	441.2	491.0	574.1	481.2	434.4	329.8	384.3	347.4	385.5	380.5	385.6	384.2	345.6	353.5	562.8	417.0	175.8
Ce	1033.7	971.6	1162.8	1204.3	1232.4	981.8	780.6	961.6	800.8	832.7	903.1	907.0	881.1	769.8	819.0	1203.9	966.0	375.7
Pr	146.3	142.9	179.4	171.3	178.1	140.9	110.6	129.2	113.6	121.1	126.9	130.8	123.6	104.2	119.6	182.7	137.0	55.3
Nd	593.4	633.5	792.1	691.2	711.2	593.8	483.2	485.3	437.4	496.1	468.2	541.1	514.4	472.5	490.1	761.2	566.0	219.5
Sm	91.4	87.0	102.8	107.5	101.3	85.9	78.1	81.1	70.2	84.0	84.0	83.7	83.8	79.4	80.4	110.4	89.0	27.4
Eu	28.6	25.4	24.0	31.9	26.2	23.4	21.0	23.6	21.9	22.3	23.8	24.6	21.4	20.7	23.0	32.0	25.0	9.1
Gd	71.6	60.2	66.5	75.0	65.4	69.7	56.0	55.7	55.2	58.7	55.2	61.0	59.6	53.8	54.3	70.7	61.0	19.3
Dy	29.6	29.1	30.8	34.0	25.4	27.1	26.4	30.4	29.0	23.3	28.3	27.8	26.3	24.1	27.2	34.9	29.0	7.5
Ho	4.9	4.3	4.2	4.6	4.1	4.3	3.8	3.7	3.5	4.2	4.3	4.0	4.5	4.1	3.5	4.9	4.0	1.1
Er	6.3	4.5	5.0	5.5	4.9	5.6	4.2	4.6	5.2	5.1	5.0	5.4	5.2	5.7	4.5	7.0	5.0	1.4
Yb	1.8	1.8	2.3	2.2	1.7	1.7	1.7	1.7	2.7	1.6	1.9	2.2	1.7	2.2	bdl	2.2	2.0	1.2
Lu	0.4	bdl	bdl	bdl	bdl	bdl	bdl	0.4	bdl	0.3	0.3	bdl	bdl	bdl	bdl	bdl	bdl	–
Sr	2383.8	2744.7	2707.8	2617.4	2377.3	2067.2	2284.0	2401.0	2222.5	2067.9	2427.0	2249.5	2363.2	2093.7	2177.3	2502.0	2315.0	485.7
Y	90.1	84.1	85.8	100.5	88.8	85.8	75.1	82.5	72.7	74.6	84.3	82.4	83.4	76.3	78.1	99.9	84.0	17.5
∑REE	2461.9	2401.6	2860.8	2901.6	2832.0	2368.6	1895.4	2161.6	1887.0	2035.0	2081.4	2173.2	2105.9	1882.1	1974.9	2972.7	2302.0	872.6

S. Brassines et al. / Lithos 83 (2005) 76–92

bearing sample at 388 ppm; Ta from 4.2 to 25 ppm. These variations appear to be directly correlated to the apatite modal abundance and to the amount of intercumulus material that is highly enriched in incompatible elements when compared to the cumulus diopside.

The ijolites have REE abundances (Σ REE \approx 1750 ppm and $(\text{La}/\text{Yb})_{\text{N}}$ varying from 20 to 53) in the range of the clinopyroxenites but they are enriched in Nb (221–437 ppm) and in Ta (47–103 ppm).

The carbonatites display large variation in trace element contents (Σ REE: 870–3617 ppm with $(\text{La}/\text{Yb})_{\text{N}}=40$ –88; Nb: 10–53 ppm, but as high as 1300 ppm for the pyrochlore-bearing carbonatite). These REE contents are well below the average calcicarbonatite of Woolley and Kempe (1989) as also observed for other Kola carbonatites (i.e., Kovdor; Verhulst et al., 2000).

All the analysed samples of the Vuoriyarvi massif plot along a well defined linear array in the Y–Ho diagram (Fig. 3), this array is characterised by a Y/Ho ratio of 22.7 ($r^2=0.987$) which is below the chondritic value of 28.7 (McDonough and Sun, 1995). In evolved systems such as alkaline intrusions and carbonatites, Nb and Ta can be fractionated by the crystallisation and the segregation of Nb- and Ta-rich minerals (Jochum et al., 1986). In the Vuoriyarvi samples, the observed perovskite and pyrochlore are indeed characterized by high to very high Nb/Ta ratio, 19 and 5000, respectively (unpublished microprobe data). The whole rock pyroxenites display homogeneous Nb/Ta ratio (9–11) that is quite comparable to the ratio of the depleted mantle (7–10; Weyer et al., 2003). One cumulus perovskite-bearing pyroxenite has a significantly higher ratio of 16. The two ijolites have lower ratio, around 5. The carbonatites have variable ratios, from 8 to 16 except sample BR30 (that contains clastic pyrochlore) that has a Nb/Ta ratio of 1300.

5.2. Apatite chemistry: evolution of the composition in the Vuoriyarvi massif

Hogarth (1989) defined 5 substitution mechanisms for apatite, the two most important ones, the belovite-type ($2\text{Ca}^{2+}=\text{Na}^{+}+\text{REE}^{3+}$) and the britholite-type ($\text{Ca}^{2+}+\text{P}^{5+}=\text{REE}^{3+}+\text{Si}^{4+}$) concern the substitution in the M crystallochemical site (Fig. 4).

Apatites from the various lithologies of the Vuoriyarvi massif have been analysed (Table 1B from major elements; Table 2 for trace elements). All analysed apatites have F content between 1.2 and 3.2 wt.% (below the stoichiometric values of 3.77 wt.%, except one analyses at 4.2 wt.%) corresponding to 0.62 to 1.67 F atoms by p.f.u.; they are thus fluorapatites. The apatites define a single, continuous evolution trend in diagrams illustrating element substitutions. In the clinopyroxenites, the apatite is Ca-rich (\approx 9.97 p.f.u.) and correlatively Na- and REE-poor (<0.07 p.f.u.) while in the carbonatites, it is significantly enriched in REE (0.08–0.22 p.f.u.; Brassinnes et al., 2003) and poorer in Ca (<9.92 p.f.u.). The apatite from the ijolites is intermediate in composition between those of the clinopyroxenites and of the carbonatites, but closer to the former. The Si content of the apatites is significantly lower in the clinopyroxenites (0.09–0.15 p.f.u.) and ijolites (0.9–0.16 p.f.u.) than in the carbonatites (0.12–0.29 p.f.u.). The F content also increases in the sequence clinopyroxenite (0.62 p.f.u.)–ijolite (0.93 p.f.u.)–carbonatite (1.67 p.f.u.). All the apatites analysed by LA-ICP-MS are rich in REEs (Fig. 5) with La_{N} values in the range 1000–10000 and Yb_{N} in the range 8–100, corresponding to strong LREE enrichment, with $(\text{La}/\text{Yb})_{\text{N}}$ varying from 49–240 and $(\text{La}/\text{Nd})_{\text{N}}>1$. There is no Eu anomaly which may be taken as evidence for oxidizing conditions.

Forty nine analyses of apatite have been performed on 13 different crystals in the clinopyroxenite VJA74. Taken altogether these analyses show a quite large range of values: Σ REE=1183–3753 ppm with $(\text{La}/\text{Yb})_{\text{N}}$ varying from 49–240; Sr=2935–4224 ppm (Fig. 5a). Five analyses performed on a single apatite crystal display some heterogeneity: the core is enriched in REE (1630 ppm) when compared to the rim (1183 ppm). Discrete, isolated apatite crystals disseminated in the sample show more variability from grain to grain (1183 to 2420 ppm of REEs; average of 29 spots: 1442 ppm; $(\text{La}/\text{Yb})_{\text{N}}$ 49 to 96). This variability could be related to the crystallisation of apatite from a more or less evolved interstitial liquid.

The polygonal apatite from segregation pockets in the clinopyroxenite (20 spots in 7 different crystals) is systematically enriched in REEs (2166 ppm to 3753 ppm; average value ($n=20$ spots): 2734 ppm with $(\text{La}/\text{Yb})_{\text{N}}=70$) when compared to discrete apatite.

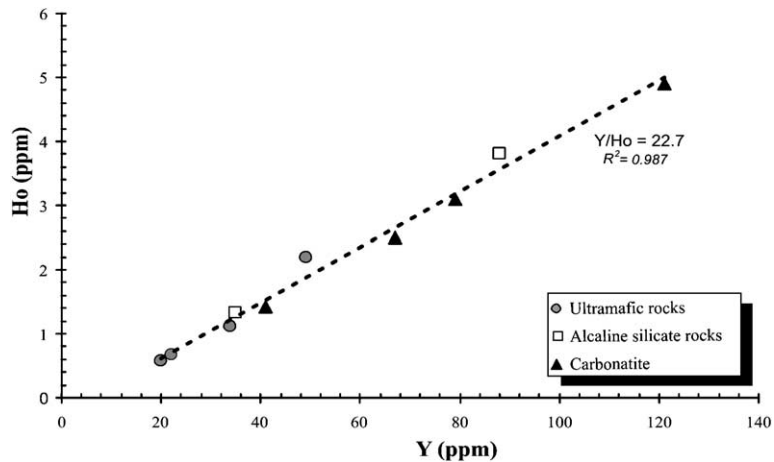


Fig. 3. Binary isovalent Y–Ho trace element diagram.

In the ijolite VJA71, 27 analyses of apatite have been made on 8 grains (Fig. 5b). The range of trace elements contents is quite narrow (Σ REE: 9176–11477 ppm, with $(La/Yb)_N$: 74 up to 145, Y: 309–572 ppm, Sr: 4371–5614 ppm). These apatites are not zoned.

The apatites of two carbonatites have been studied in detail. The apatite of the carbonatite BR18 is quite homogeneous (Fig. 5c) from grain to grain and is almost unzoned; it is rich in all trace elements (Σ REE: 10562–11942 ppm with one core analysis at 13082 ppm, $(La/Yb)_N$: 55–175, Y: 634–737 ppm, Sr: 3041–4080 ppm). The apatites from BR64 are slightly more heterogeneous (Fig. 5d); their trace element content is significantly lower: Σ REE: 1797–3430 ppm, Y: 73–111 ppm, Sr: 2067–3083 ppm. They

are slightly zoned, the REE content increases from the core to the rim of the grain (2200 to 3400 ppm, respectively). The HREE content (Yb, Lu) of these apatites is quite low, close to the limit of quantitative measurements; this explain the large range of calculated $(La/Yb)_N$ ratios (96–240). It has been shown before (Fig. 3) that the Y/Ho ratio of the whole rocks is constant in the Vuoriyarvi massif. The apatites of the clinopyroxenite display Y/Ho ratios (range: 23.4–29.7) close to the whole rock ratio and to the chondritic value. They have slight negative cerium anomaly, Ce/Ce^* ranging from 0.71 to 0.87. Similar anomalies have been observed for apatite of the early stage carbonatites (Hornig-Kjarsgaard, 1998; Bühn et al., 2001). Apatites from the ijolite have slightly lower Y/Ho ratio (24.9–20.4) and less pro-

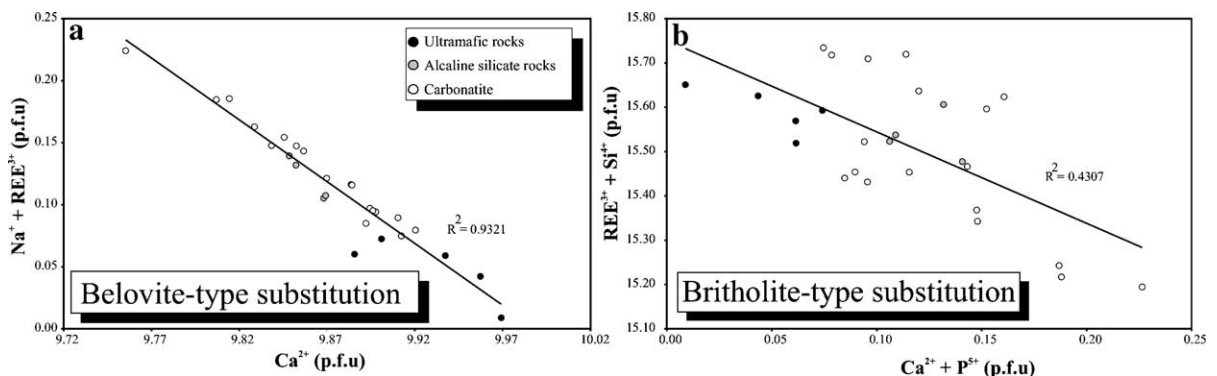


Fig. 4. Substitution schemes for apatite (in atoms per formula unit). a) Ca^{2+} versus $Na^+ + REE^{3+}$ (belovite-type); b) $Ca^{2+} + P^{5+}$ versus $REE^{3+} + Si^{4+}$ (britholite-type).

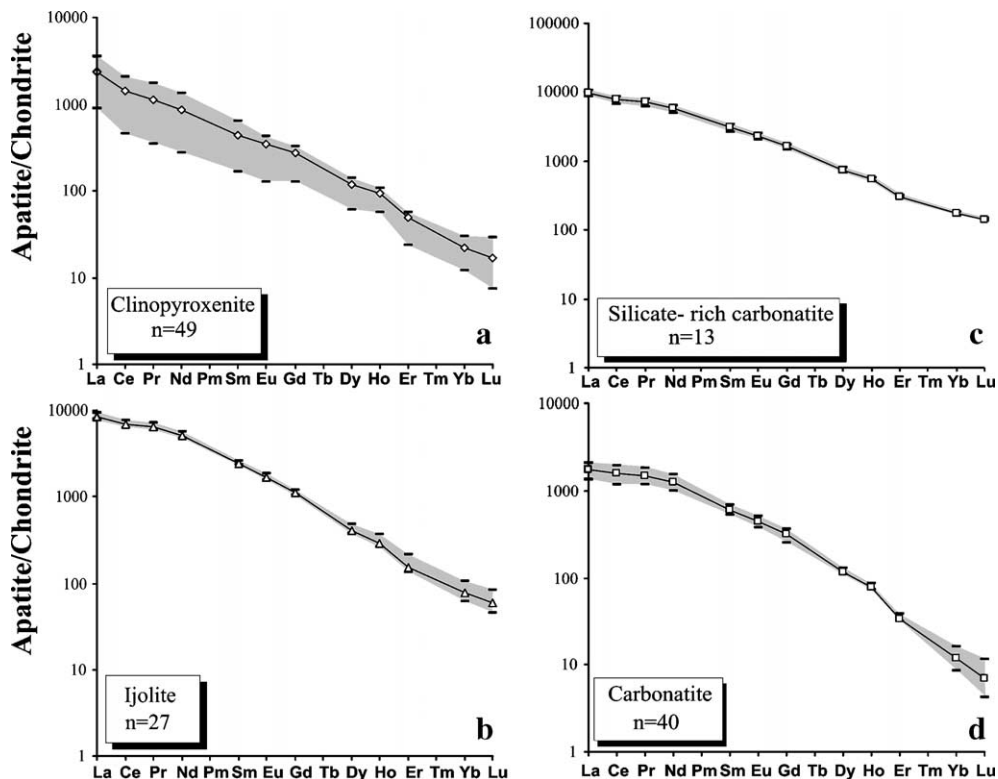


Fig. 5. Apatite chondrite normalised REE diagrams: a) in the clinopyroxenite VJA74 ($n=49$). b) in the ijolite VJA71 ($n=27$). c) in the silicate-rich carbonatite BR18 ($n=13$). d) in the carbonatite BR64 ($n=40$). For each rock type, the minimum and maximum values have been reported, as well as the average value and the range (shaded area). Normalizing values from McDonough and Sun (1995).

nounced anomaly ($Ce/Ce^*: 0.91\text{--}0.96$). The apatites from the carbonatites have still lower Y/Ho ratio, down to 16.11 and almost no Ce anomaly (Ce/Ce^* ranges from 0.87 to 1.05).

The Y/Ho ratios in the apatites and their respective whole rocks allow to test if the fractionation of apatite occurred under closed system conditions. As all the whole rock samples plot within error limits along a single line (Fig. 3), it can be stated that these elements were not fractionated during the whole magmatic evolution. Nevertheless, the Y/Ho ratio of apatite decreases from a chondritic value (27.7) in the clinopyroxenite down to ≈ 16 in the carbonatite. This significant decrease could be related to the contemporaneous fractionation of a Y-rich phase in the carbonatites. This phase could be either a Y-rich mineral, like monazite or xenotime, or fluid inclusions trapped in the carbonatite. Monazite and xenotime are frequently observed as inclusions in apatite or as outer grains on apatite surface in geo-

logical environments where fluids are abundant (Harlov and Förster, 2003). Monazite is a typical accessory mineral in the Vuorjarvi carbonatites (Kukhareenko et al., 1965; Bulakh et al., 2000). Fluids are known to complex more easily Y than Ho (Bau, 1996), so that fluid inclusions could have high Y/Ho ratios. The system had to remain closed to keep constant the ratio in the whole rock carbonatite, the high Y/Ho ratio of the monazite/xenotime or of the fluids counterbalancing the low Y/Ho ratios of the apatite.

5.3. REE distribution between apatite and the host rock: an approach to the apatite-carbonatite melt partition coefficients?

Apatite is classically interpreted as a liquidus phase in carbonatite melt (Eby, 1975; Le Bas and Handley, 1979; Eriksson et al., 1985; Le Bas, 1989; Gittins, 1989). But few trace element partition coefficients between apatite

and carbonatite melt, $D_{\text{apatite/carbonatite melt}}^{\text{REE}}$ have been reported in the literature. Two recent studies (Bühn et al., 2001; Klemme and Dalpé, 2003) give contrasting results. Böhn et al. (2001) have calculated the partition coefficients for fluorapatite in carbonatite magmas for a fractionating assemblage of calcite+fluorapatite+clinopyroxene (the latter has a minor role on the REE evolution). The estimated D values were chosen to reproduce the observed relationships in natural carbonatites from various African complexes. Böhn et al. (2001) concluded that the rare earth elements are compatible in apatite ($D_{\text{apatite/carbonatite melt}}^{\text{REE}} > 1$) and increase regularly from La to Lu, i.e., $D_{\text{La}} < D_{\text{Lu}}$. From their experimental study (at 1 GPa and 1250 °C) along the join $\text{CaCO}_3\text{--Ca}_5(\text{PO}_4)_3(\text{OH, F, Cl})$, Klemme and Dalpé (2003) measured the compositions of the apatite crystallised in carbonatite melt. The calculated partition coefficients show that the rare earth elements are incompatible in apatite, that is $D_{\text{apatite/carbonatite melt}}^{\text{REE}} < 1$. Moreover, the partition coefficients show a convex-upward pattern that means that the intermediate REE (Sm–Gd) have higher D values than the light (La–Pr) and heavy (Yb–Lu) REE. Similar convex-upward patterns have been obtained for apatite from various silicate melts (Watson and Green, 1981), but in all silicate systems, the REEs are compatible in apatite ($D_{\text{apatite/carbonatite melt}}^{\text{REE}} > 1$). Watson and Green (1981) noted that the apatite/melt REE partition coefficients significantly decrease with decreasing silica activity, from a granite melt to a basanite melt. Klemme and Dalpé (2003) suggest that their very low (< 1) D values can be related to the very low (close to zero) silica activity of the carbonatite melt. Another explanation could be proposed: besides melt composition, P and T can have a profound effect on mineral–melt partitioning (see review in Blundy and Wood, 2003). The variations of the D values with pressure can lead to contrasting results (either decreasing or increasing D with increasing P) depending on the material (i.e., Chamarro et al., 2002 for clinopyroxene–silicate melt). The accommodation of REE in apatite with increasing P is not known.

The field relations and the petrographic features of carbonatite BR64 suggested that it could be interpreted as a “quenched melt”. Using the average composition of the apatite and the REE partition coefficients (both minimum and maximum values

Table 3
Estimated distribution coefficients (REE+Y) between apatite and carbonatite host rock and partition coefficients from the literature

	La	Ce	Pr	Nd	Sm	Eu	Gd	Dy	Ho	Y	Er	Yb	Lu
BR 64	Ap./C. h. rek.	4.1	4.7	5.4	6.1	6.1	5.6	4.4	3.8	2.1	2.1	1.0	–
BR 18	Ap./C. h. rek.	18.1	15.9	20.1	23.6	23.9	19.0	17.0	17.2	12.5	9.2	8.4	8.4
Watson and Green (1981)	Ap./basan.	2.6	–	–	–	4.5	–	4.0	–	–	–	1.8	–
Böhn et al. (2001)	Ap./C. melt	0.9–1.5	1.8–2.5	2.4–3.4	2.8–4.5	3.6–6.5	4.1–7.1	4.5–7.5	5.1–8.1	5.4–8.4	–	5.6–8.7	6.2–10
Klemme and Dalpé (2003)	Ap./C. melt	0.23–0.33	0.19–0.40	0.31–0.45	–	0.43–0.55	–	0.49–0.58	–	–	–	–	0.23–0.34
Klemme et al. (1995)	Cpx/C. melt	0.07	0.09	0.11	0.13	0.22	0.26	0.29	–	0.3	0.41	–	–
Nagasawa et al. (1980)	Per./Alk. bslt.	2.62	–	–	2.70	2.00–2.34	–	–	–	–	1.00	0.49	0.41

Watson and Green (1981) for a basanite, Böhn et al. (2001) and Klemme and Dalpé (2003) for carbonatite melts.

Ap.: apatite, C. h. rek: carbonatite host rock, basan: basanite, C. melt: carbonatite melt, Cpx: clinopyroxene, Per: perovskite and Alk. Bslt.: alkali basalt.

were used) of Klemme and Dalpé (2003) and Bühn et al. (2001) (see Table 3), the range of REE concentrations in the carbonatite melt in equilibrium with apatite has been calculated. Obviously, the liquid calculated with the low partition coefficients values of Klemme and Dalpé (2003) has a much higher REE content (1263–1813 ppm La) than the one obtained with the D values of Bühn et al. (2001) (278–463 ppm La). The $(\text{La}/\text{Yb})_{\text{N}}$ ratios are also different (≈ 140 and ≈ 950 , respectively) because the variation of the D_{REE} values with atomic number is very different in the two sets of partition coefficients. The two ranges of calculated carbonatite liquid composition are not overlapping but they, nevertheless, both fall in the range of the carbonatite analyses of Woolley and Kempe (1989). We have tried to estimate the partition coefficients from our own data. Strictly speaking, we estimate the REE distribution between apatite and host carbonatite (as an approximation of carbonatite melt). The contribution of the apatite to the bulk rock REE budget has been subtracted in order to obtain the REE content of the host carbonatite ((whole rock REE content – (apatite REE content * apatite modal percentage)). The average composition of the 40 analysed spots (including core and rim analyses) have been used. The modal abundance of apatite is derived from the P_2O_5 content of the whole rocks (see Table 1); it is 8.1%. The estimated partition coefficients, $D_{\text{apatite/carbonatite melt}}^{\text{REE}}$ are given in Table 3 and compared with the values of Bühn et al. (2001) and Klemme and Dalpé (2003). These partition coefficients are plotted (Fig. 6) in function of the cation radius (in six fold coordination from Shannon, 1976). The law of partitioning is near-parabolic (as first noted by Onuma et al., 1968) which is typical for partition coefficients in the lattice-strain model (Blundy and Wood, 1994). The regression curve does not fit very well for the heavy REE (Er–Yb) and Y. In fact, these elements have quite low contents, close to the quantification limits of the LA-ICP-MS instrument used. Our estimated partition coefficients are quite close to those obtained by Watson and Green (1981) for apatite crystallising from a basanite melt. Interestingly, basanite is strongly silica-undersaturated like the olivine-bearing melanephelinite (or melmelilitite) that is considered as the parental magma of the ultramafic, alkaline and carbonatite complex (i.e., Veksler et al., 1998a).

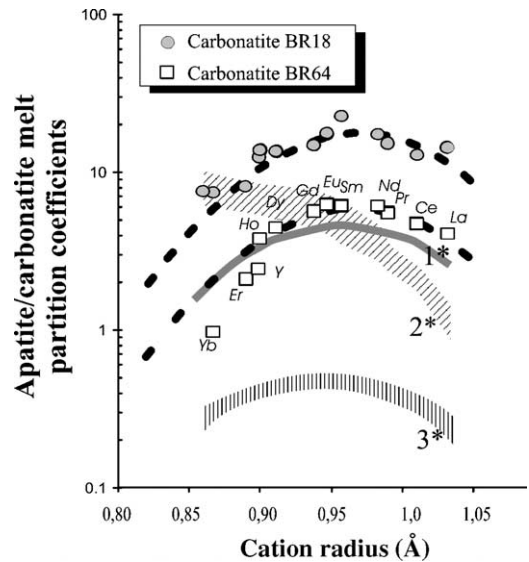


Fig. 6. Estimated distribution coefficients (REE+Y) versus cation radii (in six fold coordination from Shannon, 1976) between apatite and carbonatite host rock. Comparison with the data of Watson and Green (1981) for a basanite (1*), Bühn et al. (2001) and Klemme and Dalpé (2003) for carbonatite melts (2* and 3*, respectively).

The same procedure has been applied to the carbonatite BR18, even if it is probably not a quenched melt. This rock is significantly enriched in REE ($\Sigma\text{REE}=2163$ ppm) and in silica (7 wt.% SiO_2) when compared to BR64. The D values obtained are higher than for BR64 but the profiles are similar.

The two curves obtained for the apatite/host carbonatite of Vuoriyarvi are convex-upward (Fig. 6) and centered on the middle rare earth elements, the maximum of the curve corresponds to the cation radius of Sm. The apatite REE partition coefficient values for the Vuoriyarvi carbonatites are all higher than 1 (4.1 for La; 6.1 for Sm and 1.0 for Yb for BR64).

6. Discussion on the petrogenetic link between the ultramafic cumulates, the alkaline silicate rocks and the carbonatites

In the Vuoriyarvi massif, as well as in many other massifs of the Kola province, the ultramafic cumulates (clinopyroxenite), the alkaline silicate rocks and the carbonatites are closely related in space and time. Is this association really a coincidence?

Isotope geochemistry can shed some light on this problem. For the large and complex massifs of the Kola Peninsula (i.e., Khibiny, Kovdor, Turij Mys, etc. . .) several papers (Kramm, 1993; Kramm and Kogarko, 1994; Zaitsev and Bell, 1995; Verhulst et al., 2000; Dunworth and Bell, 2001) have shown that the ultramafic rocks, the ijolites–melteigites and the carbonatites do not display exactly the same initial Sr–Nd isotopic composition suggesting that they are not strictly cogenetic even if most samples plot in the depleted mantle quadrant of the Sr–Nd anticorrelation diagram, close to the source of the OIBs. In fact, for the Kovdor massif (Verhulst et al., 2000), the carbonatites show quite a large range of isotopic compositions but all the values plot in the depleted quadrant. As it is very difficult to contaminate carbonatites because of their very high Sr and Nd content (much higher than in crustal materials), this spread of composition suggests that the Kovdor intrusion behaves as a complex, open system implying several discrete magma pulses from the mantle. It has been shown experimentally (Wyllie and Huang, 1976; Eggler, 1978; Wallace and Green, 1988; Green and Wallace, 1988; Wyllie and Lee, 1998) that carbonatite can be formed directly by very low degrees of partial melting of a carbonated upper mantle source. The ultramafic cumulates and the melilitolites are isotopically compatible with this model. The ijolites–melteigites, on the contrary, have more scattered isotopic compositions, with both positive and negative $\epsilon\text{Nd}_{380 \text{ Ma}}$ values pointing to some contamination by crustal material and/or to magma mixing. Contrary to what has been observed for the large Kola intrusions, the small Vuoriyarvi massif presents more uniform isotopic composition: the clinopyroxenites, ijolites and carbonatites have $^{87}\text{Sr}/^{86}\text{Sr}_{380 \text{ Ma}}$ ratios in the narrow range 0.70303–0.70318 and $\epsilon\text{Nd}_{380 \text{ Ma}}$ in the range +3.6 to +6.1 (Balaganskaya et al., 2001; Zaitsev et al., 2002; our unpublished data). Only a biotite–amphibole–calcite vein analysed by Balaganskaya et al. (2001) has a significantly different isotopic compositions, 0.70341 and +1.8. This sample is in fact not a true carbonatite, it is more comparable to a fenite. This narrow range of isotopic composition is in favour of a single batch of homogeneous mantle-derived melt that crystallised and evolved in a closed system. The Nb/Ta ratio of the least evolved samples in the Vuoriyarvi massif (clinopyroxenite) is compa-

rable to the depleted mantle source values (7–10; Weyer et al., 2003). All the lithologies observed in the Vuoriyarvi massif are petrogenetically linked; they have the same age, the same initial Sr–Nd isotopic composition. Nevertheless, the nature of this petrogenetic link still needs to be clarified: it could be the liquid immiscibility between a carbonatite melt and an alkaline silicate melt (Lee and Wyllie, 1996; Kjarsgaard and Hamilton, 1998, Veksler et al., 1998b; Stoppa et al., 2005) or a simple fractional crystallisation process operating on a single magma batch derived the depleted mantle (Lee and Wyllie, 1998). There is no evidence for immiscibility between an alkaline silicate melt and carbonatite, neither in the field nor in the geochemical data. The spherulitic textures described by Lapin and Vartiainen (1983) are interpreted in terms of liquid immiscibility between sövite and phoscorite (forsterite–magnetite rocks). These rocks due to their specific structures may also be interpreted as fluid-explosive breccias which were discovered and studied in the Kovdor alkaline-ultramafic massif (Balaganskaya, 1994). Moreover, the apatites from the ultramafic rocks, the ijolites and the early carbonatites display continuous geochemical trends, like enrichment in Na+REE (Fig. 4), a decrease in the Y/Ho ratio in agreement with an evolution by fractional crystallisation. The increase in REE content of apatite in the sequence clinopyroxenite–ijolite–carbonatite implies that the global REE partition coefficients for the fractionating mineral assemblage is lower than 1. During the first fractionation stage, the main phases that crystallise are clinopyroxene and apatite with perovskite in subordinate amounts. Using the values of Klemme et al. (1995) for the partition coefficients of REE between clinopyroxene and carbonatite melt, our average estimated values for apatite (Table 3) and the value of Nagasawa et al. (1980) for the perovskite, it can be shown that for a fractionating assemblage varying from 98% cpx+1% ap+1% per to 94% cpx+5% ap+1% per, the global D_{REE} varies from 0.14 to 0.30.

The variation of REE content during the magmatic evolution of the late carbonatite stage of differentiation is difficult to model because carbonatite veins and phoscorite stocks (or bodies) are intimately related in the field. Moreover, phoscorites are generally very coarse-grained, some can be strongly enriched in

apatites and could be formed by pulses of intensive apatite crystallisation (Bühn et al., 2001).

7. Conclusion

In the Vuoriyarvi massif, ultramafic cumulates (clinopyroxenites), alkaline silicate rocks and carbonatites are spatially and temporally associated. Apatite is subhedral to euhedral in ultramafic cumulates and ijolites; it is in equilibrium with the intercumulus liquid. Some carbonatites, which are mainly found as thin dykes or sheets are tentatively interpreted as liquids. They are rich in euhedral apatites. Clinopyroxenites display a large range of trace element content that is directly related to the proportion of interstitial liquid. Carbonatites have variable trace element contents depending mainly on their apatite and pyrochlore modal proportions. The ijolites are more homogeneous. All the whole rock samples plot along well-defined arrays in the Y–Ho diagram suggesting that they are all cogenetic. The Sr–Nd initial isotopic compositions are well clustered for all the lithologies and point to a closed system evolution of a single batch of mantle-derived magma. The increase of Na+REE and the decrease of the Y/Ho ratio from the clinopyroxenites to the carbonatites are in agreement with an evolution by fractional crystallisation. Distribution coefficients between apatite and host carbonatite, interpreted as an approximation of the true partition coefficients, have been estimated for a carbonatite from the Neskevara conical-ring-like vein system (sample BR64). All the *D* values are higher than 1 (the REE are compatible in apatite) and display a convex-upward pattern when plotted against ionic radii, pointing to a higher compatibility for the middle rare earth elements.

Acknowledgments

This work has been initiated by an INTAS grant project No. 94-2621 to D.D. Dr. I. Tolstikhin (Apatity, Russia) started the collaboration between the Belgian and the Russian teams. Prof. F. Mitrofanov (Kola Center, Apatity, Russia) allowed us to study the Kola alkaline province. Drs. V. Vetrin and V. Nivin are warmly thanked for the perfect organization of the

field trips. We thank Dr. Ohnenstetter (CRPG, Nancy, France) for the supervision of the microprobe determinations and Dr. L. André and Nicolas Coussaert (Musée Royal de l'Afrique Centrale, Belgium) for the LA-ICP-MS analyses. The constructive reviews of Dr S. Klemme and of an anonymous reviewer as well as the suggestions and comments of Dr F. Wall (Guest Editor) are gratefully acknowledged.

References

- André, L., Aschepkov, I.V., 1996. Acid leaching experiments on the mantle-derived Vitim clinopyroxenes: implications for the role of clinopyroxenes in the mantle processes. In: Demaiffe, D. (Ed.), *Petrology and Geochemistry of Magmatic Suites of Rocks in the Continental and Oceanic Crusts*. ULB-MRAC, pp. 321–336.
- Balaganskaya, E.G., 1994. Breccias of the Kovdor phoscorite–carbonatite deposit of magnetite and their geological meaning. *Proceedings of the All-Russia Mineralogical Society*, vol. 2, pp. 24–36 (in Russian).
- Balaganskaya, E., Downes, H., Subbotin, V., Liferovich, R., Beard, A., 2001. Kola carbonatites: new insights into their origin as shown by a Sr, Nd and geochemical study of the Vuoriyarvi Massif, NE Baltic Shield, Russia. *Abstr., Journ. Afric. Earth Sci.* 32 (1), A11.
- Balagansky, V.V., Basalava, A.A., Belyaev, O.A., Pozhilenko, V.I., Radchenko, A.T., Radchenko, M.K. 1996. Geological map of the Kola region (north-eastern Baltic shield) scale 1:500,000. In: Mitrofanov, F.P., Radchenko, A.T., Gillen, C. (Eds.), *Apatity*.
- Bau, M., 1996. Controls on the fractionation of isovalent trace elements in magmatic and aqueous systems: evidence from Y/Ho, Zr/Hf and lanthanide tetrad effect. *Contrib. Mineral. Petrol.* 123, 323–333.
- Blundy, J., Wood, B., 1994. Prediction of crystal melt partition coefficients from elastic moduli. *Nature* 372, 452–454.
- Blundy, J., Wood, B., 2003. Partitioning of trace elements between crystals and melts. *Earth Planet. Sci. Lett.* 210, 383–397.
- Brassinnes, S., Demaiffe, S., Balaganskaya, E., Downes, H., 2003. New mineralogical and geochemical data on the Vuoriyarvi ultramafic, alkaline and carbonatitic complex (Kola Region, NW Russia). *Period. Mineral.* 72, 79–86.
- Bulakh, A.G., Nesterov, A.R., Zaitsev, A.N., Pilipiuk, A.N., Wall, F., Kirillov, A.S., 2000. Sulfur-containing monazite—(Ce) from late-stage mineral assemblages at the Kandaguba and Vuoriyarvi carbonatite complexes, Kola peninsula, Russia. *N. Jb. Miner. Mh.* 5, 217–233.
- Bühn, B., Wall, F., Le Bas, M.J., 2001. Rare-earth element systematics of carbonatitic fluorapatites, and their significance for carbonatite magma evolution. *Contrib. Mineral. Petrol.* 141, 572–591.
- Chamarro, E.M., Brooker, R.A., Wartho, J.-A., Wood, B.J., Kelley, S.P., Blundy, D., 2002. Ar and K partitioning between clinopyr-

- oxene and silicate melt to 8 GPa. *Geochim. Cosmochim. Acta* 66, 507–519.
- Dunworth, E.A., Bell, K., 2001. The Turij Massif, Kola Peninsula, Russia: isotopic and geochemical evidence for a multi-source evolution. *J. Petrol.* 42, 377–405.
- Eby, G.N., 1975. Abundance and distribution of rare-earth elements and yttrium in the rocks and minerals of the Oka carbonatite complex, Quebec. *Geochim. Cosmochim. Acta* 39, 597–620.
- Eggler, D.H., 1978. The effect of CO₂ upon partial melting of peridotite in the system Na₂O–CaO–Al₂O₃–MgO–SiO₂–CO₂ to 35 kb with analysis of melting in a peridotite–H₂O–CO₂ system. *Am. J. Sci.* 278, 305–343.
- Eriksson, S.C., Fourie, P.J., De Jager, D.H., 1985. A cumulate origin for the minerals in clinopyroxenite of the Phalaborwa Complex. *Trans. Geol. Soc. S. Afr.* 88, 207–214.
- Gittins, J., 1989. The origin and evolution of carbonatite magmas. In: Bell, K. (Ed.), *Carbonatites: Genesis and Evolution*. Unwin Hyman, London, pp. 580–600.
- Gittins, J., Harmer, R.E., 2003. Myth and reality of the carbonatite–silicate rock “association”. *Period. Mineral.* 72, 19–26.
- Gogol, O., Delinitzin, A., 1999. New Rb–Sr data for Kola alkaline province. *Proc. 10th Kratz Conf., Apatity*, pp. 43–47 (in Russian).
- Green, D.H., Wallace, M.E., 1988. Mantle metasomatism by ephemeral carbonatite melts. *Nature* 336, 459–462.
- Harlov, D.E., Förster, H.-J., 2003. Fluid-induced nucleation of (Y+REE)-phosphate minerals within apatite: nature and experiment: Part II. Fluorapatite. *Am. Mineral.* 88, 1209–1229.
- Henoc, J., Tong, M., 1978. Automatisation de la microsonde. *J. Microsc. Spectrosc. Electr.* 3, 247–254.
- Hogarth, D.D., 1989. Pyrochlore, apatite and amphibole: distinctive minerals in carbonatite. In: Bell, K. (Ed.), *Carbonatites: Genesis and Evolution*. Unwin Hyman, London, pp. 105–148.
- Hornig-Kjarsgaard, I., 1998. Rare earth elements in sövitic carbonatites and their mineral phases. *J. Petrol.* 39, 2105–2122.
- Jochum, K.P., Seufert, H.M., Spettel, B., Palme, H., 1986. The solar system abundances of Nb, Ta and Y, and the relative abundances of refractory lithophile elements in differentiated planetary bodies. *Geochim. Cosmochim. Acta* 50, 1173–1183.
- Kapustin, Yu.L., 1980. *Mineralogy of Carbonatites*. Amerind Publishing Co. 259 pp.
- Kjarsgaard, B.A., Hamilton, D.L., 1998. The genesis of carbonatite by immiscibility. In: Bell, K. (Ed.), *Carbonatites: Genesis and Evolution*. Unwin Hyman, London, pp. 388–404.
- Klemme, S., Dalpé, C., 2003. Trace-element partitioning between apatite and carbonatite melt. *Am. Mineral.* 88, 639–646.
- Klemme, S., van der Laan, S.R., Foley, S.F., Günther, D., 1995. Experimentally determined trace and minor element partitioning between clinopyroxene and carbonatite melt under upper mantle conditions. *Earth Planet. Sci. Lett.* 133, 439–448.
- Kogarko, L.N., 1987. Alkaline rocks of the eastern part of the Baltic Shield (Kola Peninsula). In: Fitton, J.G., Upton, B.G.J. (Eds.), *Alkaline Igneous Rocks*, Geol. Soc. Special Publication, vol. 30, pp. 531–544.
- Kogarko, L.N., Kononova, V.A., Orlova, M.P., Woolley, A.R., 1995. *Alkaline Rocks and Carbonatites of the World: Part 2. Former USSR*. Chapman and Hall, London. 225 pp.
- Kramm, U., 1993. Mantle components of carbonatites from the Kola alkali province, Russia and Finland: a Nd–Sr study. *Eur. J. Mineral.* 5, 985–989.
- Kramm, U., Kogarko, L., 1994. Nd and Sr isotope signatures of the Khibiny and Lovozero apatitic centres, Kola Alkaline Province, Russia. *Lithos* 32, 225–242.
- Kramm, U., Kogarko, L., Kononova, V.A., Vartiainen, H., 1993. The Kola Alkaline Province of the CIS and Finland: precise Rb–Sr ages define 380–360 Ma age range for all magmatism. *Lithos* 30, 33–44.
- Kratz, K.O., Glebovitskiy, R.V., Bilinskiy, V.L., Duk, I.B., Litvinenko, E.V., Sharkov, G.A., Porotova, S.A., Ankudinov, L.N., Platonenkova, L.N., Kokorina, L.K., Lazarev, Y.K., Platonova, A.P., Koshekin, B.I., Lvukashev, A.D., Stelkov, S.A., 1978. *The Earth's Crust in the Eastern Part of the Baltic Shield*. Nauka, Leningrad. 232 pp. (in Russian).
- Kukhareenko, A.A., Orlova, M.P., Boulakh, A.G., Bagdasarov, E.A., Rimskaya-Korsakova, O.M., Nefedov, E.I., Ilinskiy, G.A., Sergeev, A.S., Abakumova, N.B., 1965. *The Caledonian Complex of Ultrabasic Alkaline Rocks of the Kola Peninsula and North Karelia*. Nedra, Moscow. 772 pp. (in Russian).
- Lapin, A.V., Vartiainen, V.H., 1983. Orbicular and spherulitic carbonatites from Sokli and Vuoriyarvi. *Lithos* 16, 53–60.
- Le Bas, M.J., 1989. Diversification of carbonatite. In: Bell, K. (Ed.), *Carbonatites: Genesis and Evolution*. Unwin Hyman, London, pp. 428–445.
- Le Bas, M.J., Handley, C., 1979. Variation in apatite composition in ijolitic and carbonatitic igneous rocks. *Nature* 279, 54–56.
- Lee, W.-J., Wyllie, P.-J., 1996. Liquid immiscibility in the join NaAlSi₃O₈–CaCO₃ to 2.5 GPa and the origin of calciocarbonatite magmas. *J. Petrol.* 37, 1125–1152.
- Lee, W.-J., Wyllie, P.-J., 1998. Petrogenesis of carbonatite magmas from mantle to crust constrained by the system CaO–(MgO+FeO*)–(Na₂O+K₂O)–(SiO₂+Al₂O₃+TiO₂)–CO₂. *J. Petrol.* 39, 495–517.
- McDonough, W.F., Sun, S.-S., 1995. The composition of the Earth. *Chem. Geol.* 120, 223–253.
- Mitrofanov, F.P. (Ed.), 1995. *Geology of the Kola Peninsula*, Kola Science Center. Apatity, 145 pp.
- Nagasawa, H., Schreiber, H.D., Morris, R.V., 1980. Experimental mineral/liquid partition coefficients of the rare earth elements (REE), Sc and Sr for perovskite, spinel and melilite. *Earth Planet. Sci. Lett.* 46, 431–437.
- Onuma, N., Higuchi, H., Wakita, H., Nagasawa, H., 1968. Trace element partition between two pyroxenes and the host lava. *Earth Planet. Sci. Lett.* 5, 47–51.
- Russel, H.D., Hiemstra, S.A., Groenvald, D., 1954. The mineralogy and the petrography of the carbonatite. *Trans. and Proceed. Geol. Soc. South Africa*, pp. 197–208.
- Shannon, R.D., 1976. Revised effective ionic radii and systematic studies of inter atomic distances in halides and chalcogenides. *Acta Crystal* 32, 751–767.
- Stoppa, F., Rosatelli, G., Wall, F., Jeffries, T., 2005. Geochemistry of carbonatitesilicate pairs in nature: a case history from central Italy. *Lithos* 85, 26–47. doi:10.1016/j.lithos.2005.03.026 (this volume).

- Timmerman, M.J., Daly, J.S., 1995. Sm–Nd evidence for Late Archean crust formation in the Lapland–Kola mobile belt, Kola Peninsula, Russia and Norway. *Precambrian. Res.* 72, 97–107.
- Veksler, I.V., Nielsen, T.F.D., Sokolov, S.V., 1998a. Phase equilibria in the silica-undersaturated part of the $\text{KAlSiO}_4\text{--Mg}_2\text{SiO}_4\text{--Ca}_2\text{SiO}_4\text{--SiO}_2\text{--F}$ system at 1 atm and the lamite-normative trend of melt evolution. *Contrib. Mineral. Petrol.* 131, 347–363.
- Veksler, I.V., Petibon, C., Jenner, G.A., Dorfman, M., Dingwell, D.B., 1998b. Trace element partitioning in immiscible silicate–carbonate liquid systems: an initial experimental study using a centrifuge autoclave. *J. Petrol.* 39, 2095–2104.
- Verhulst, A., Balaganskaya, E., Kimarsky, Y., Demaiffe, D., 2000. Petrological and geochemical (trace elements and Sr–Nd isotopes) characteristics of the Paleozoic Kovdor ultramafic, alkaline and carbonatite intrusion (Kola Peninsula, NW Russia). *Lithos* 51, 1–25.
- Wallace, M.E., Green, D.H., 1988. An experimental determination of primary carbonatite magma composition. *Nature* 335, 343–348.
- Watson, E.B., Green, T.H., 1981. Apatite/liquid partition coefficients for the rare earth elements and strontium. *Earth Planet. Sci. Lett.* 56, 405–421.
- Weyer, S., Münker, C., Mezger, K., 2003. Nb/Ta, Zr/Hf and REE in the depleted mantle: implications for the differentiation history of the crust–mantle system. *Earth Planet. Sci. Lett.* 205, 309–324.
- Woolley, A.R., 2003. Igneous silicate rocks associated with carbonatites: their diversity, relative abundances and implications for carbonatite genesis. *Period. Mineral.* 72, 9–17.
- Woolley, A.R., Kempe, D.R.C., 1989. Carbonatites: nomenclature, average chemical compositions, and element distribution. In: Bell, K. (Ed.), *Carbonatites: Genesis and Evolution*. Unwin Hyman, London, pp. 1–14.
- Wyllie, P.J., Huang, W.-L., 1976. Carbonation and melting relations in the system CaO--MgO--SiO_2 at mantle pressures with geophysical and petrological applications. *Contrib. Mineral. Petrol.* 54, 79–107.
- Wyllie, P.J., Lee, W.-L., 1998. Model system controls on conditions for formation of magnesiocarbonatite and calciocarbonatite magmas from the mantle. *J. Petrol.* 39, 1885–1893.
- Zaitsev, A.N., Bell, K., 1995. Sr and Nd isotope data of apatite, calcite and dolomite as indicators of source and the relationships of phoscorites and carbonatites from the Kovdor massif, Kola Peninsula, Russia. *Contrib. Mineral. Petrol.* 121, 324–335.
- Zaitsev, A.N., Demény, A., Sindern, S., Wall, F., 2002. Burbankite group minerals and their alteration in rare earth carbonatites—source of elements and fluids (evidence from C–O and Sr–Nd isotopic data). *Lithos* 62, 15–33.